Thin Solid Films 582 (2015) 124–127

Contents lists available at ScienceDirect

Thin Solid Films

journal homepage: www.elsevier.com/locate/tsf

Improving CdS/CdTe thin film solar cell efficiency by optimizing the physical properties of CdS with the application of thermal and chemical treatments

J.M. Flores-Marquez [a], M.L. Albor-Aguilera [a], Y. Matsumoto-Kuwabara [b], M.A. Gonzalez-Trujillo [c,*], C. Hernandez-Vasquez [a], R. Mendoza-Perez [d], G.S. Contreras-Puente [a], M. Tufiño-Velazquez [a]

[a] ESFM-IPN, Depto. Fisica, U.P.A.L.M., Zacatenco, Mexico D.F. 07738, Mexico
[b] CINVESTAV-SEES-IPN, Av. IPN 2508, Zacatenco, Mexico D.F. 07360, Mexico
[c] ESCOM—IPN, Formacion Basica, U.P.A.L.M., Zacatenco, Mexico D.F. 07738, Mexico
[d] UACM, Av. Prol. San Isidro 151, San Lorenzo Tezonco, Mexico D.F. 09790, Mexico

ARTICLE INFO

Available online 25 October 2014

Keywords:
Cadmium sulfide
Chemical bath deposition
Solar cells

ABSTRACT

CdS polycrystalline thin films have been used as a window layer in CdTe, Cu(In,Ga)Se_2 and Cu_2ZnSnS_4 solar cells; the specific optical and electrical properties of the CdS-partner play an important role in the photovoltaic device performance, so that one of the problems to be solved is to reduce the pin-hole density and intergrain cavities on the CdS surface. SnO_2:F/soda-lime glass substrates (FTO) were treated with HCl, Ar and O_2. CdS films were deposited on FTO substrates by using the chemical bath deposition technique and then CdS thin films were thermally annealed on $CdCl_2$, Ar atmospheres and muffle at atmospheric ambient. Optical and morphological measurements revealed that the HCl treatment improves the CdS growth because the defect levels were reduced while the grain size is increased. The processed CdS-thin films were applied on CdTe solar cells and the photovoltaic efficiency was about 12% when the CdS thin films were thermally annealed in muffle at atmospheric ambient.

1. Introduction

CdS has been widely used as the window material in CdTe, Cu(In,Ga)Se_2, and Cu_2ZnSnS_4 thin film solar cells technology. Solar cell efficiency is influenced by the charge transport in the heterojunction of the window and absorber materials when they are fabricated. In order to achieve high efficiencies CdS must be free of defects such as intergrain cavities and pin-holes [1]. The CdS/CdTe solar cell efficiency record is 20.4% at laboratory level, and 16.1% in solar panels [2,3]. These efficiencies, however, are well below the calculated theoretical limit of about 30% [4]. The ZnO/CdS/Cu(In,Ga)Se_2 thin-film solar cells have a record efficiency of 20.8% and the record efficiency of the based $Cu_2ZnSn(S,Se)_4$ solar cells is close to 11.1% value [5,6].

Thin film solar cell technology requires deposition methods that ensure simplicity, low production cost and high efficiencies. The chemical bath deposition technique (CBD) has demonstrated to be a simple and low cost technique to prepare high quality CdS films as optical window for solar cells. Different approaches can be followed to improve the physical properties of CBD-CdS thin films for technological applications. In this work we studied the impact of several thermal and chemical treatments on the physical properties of the CdS thin films deposited by the CBD technique on different substrates, varying the CdS growth parameters, with the aim to optimize CdS thin film physical properties to be used in thin film solar cell technology.

2. Experimental details

CdS semiconductor thin films were deposited on SnO_2:F/soda-lime glass substrates (FTO) by CBD technique. The $CdCl_2$ (0.1 M), and $SC(NH_2)_2$ (0.3 M) were used as precursor solutions for the Cd and S ion to ion deposition, respectively. NH_4Cl (0.2 M) and NH_4OH(2 M) were used to promoted the formation of complex compounds and pH values. Some substrates were treated with HCl (0.1 M) during 45 min, and others were annealed using different atmospheres (Ar and O_2) at 500 °C. The CdS thin films (bi-layers; obtained with two 30 nm CdS films subsequently deposited) in areas of 4 cm^2 were obtained using a deposition time of 8 min at 76 ± 2 °C for all cases [1]. CdS thin films were annealed in a muffle and Ar atmospheres at 450 °C during 60 min; other samples were thermally annealed in $CdCl_2$ at 350 °C by 30 min.

CdS/CdTe solar cells were completed using CdTe thin films (4 μm of thickness) deposited by the close space vapor transport technique. Cu and Au (20 Å and 100 nm, respectively) were deposited as back contact with a circular area of 0.078 cm^2.

The structural characteristics of the samples were determined by the grazing incidence X-ray diffraction (GI-XRD) patterns, by means of a Panalytical X'pert Pro system. The Cu-$K_{\alpha 1}$ at 45 kV and 20 mA was

* Corresponding author.

http://dx.doi.org/10.1016/j.tsf.2014.10.070
0040-6090/

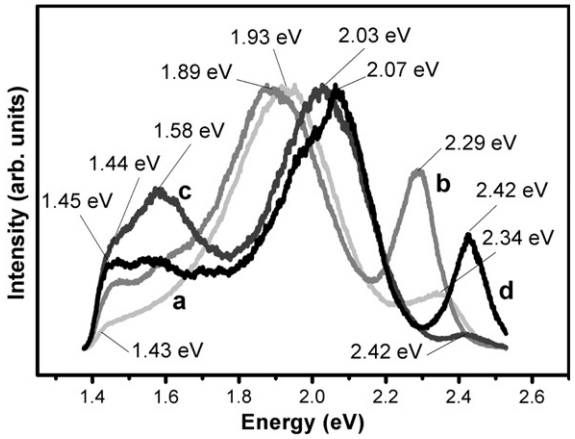

Fig. 1. Photoluminescence spectra at 10 K (a) CdS/FTO, (b) CdS/FTO_{HCl}, (c) CdS/FTO_{O2} and (d) CdS/FTO_{Ar}.

used as X-ray source. Because the films were very thin, about 60 nm, the grazing angle diffraction is used with incident light angle fixed at 1°. The scan step interval is chosen to be 0.04°, and scan time is 0.5 sec. Comparing the peak positions and relative intensities with standard data, we can determine the components on the surface and their structures.

The thickness of the layer was measured with a step profiler with 15 Å to vertical resolution (AMBIOS TECHNOLOGY XP-100). Morphological analysis was made using a scanning electron microscope (SEM) Auriga-Zeiss model with a voltage of 5 kV, allowing a resolution of 2 nm. Elemental analysis was obtained using an EDAX detector with a spectral resolution of 129 eV and 0.001 cps/eV coupled to SEM using an acceleration voltage of 10 kV. *K*-line and *L*-line were used to detect (C, O and S) and (Cd and Sn) respectively. We used a work distance of 7 mm and a magnification of 10,000×. A PB-ZAF correction method was applied. Optical properties were obtained using a Shimadzu UV 2401-PC spectrometer. The current (I) vs. voltage (V) characterization was made with a 91160 Oriel-Newport simulator with an AM-1.56 filter, which simulates a 1.5 air mass solar radiation spectrum with 100 mW/cm^2 intensity.

3. Results and discussion

3.1. Morphological and optical properties

In a previous work a study of the different treatments of FTO substrates has been presented [1]. From these studies, FTO substrates without treatment showed an average grain size of about 35 nm; on the other hand the FTO substrates treated with HCl showed a decreasing of the grain size at around 18 nm. It's promoting an increase of capture centers (nucleation points We determined that the CdS growth using FTO treated with HCl (CdS/FTO_{HCl}) increases the CdS grain size [1]. In this way and with the purpose of improving the crystalline properties of CdS thin films, the samples were subjected to different thermal treatments. All deposited CdS thin films have an average thickness of around 60 nm.

The photoluminescence spectrum of CdS/FTO_{HCl} shows a peak with large intensity located at 2.29 eV corresponding with sulfur interstices (see Fig. 1(b)); on the other hand Fig. 1d shows a spectrum related with CdS films deposited on FTO treated with Ar (CdS/FTO_{Ar}). In this case, a peak located at 2.42 eV appears; it correspond with an electronic recombination due to band-to-band transition. Fig. 1(a, c) corresponds with CdS thin films deposited on FTO substrates without treatment (CdS/FTO) and treated with O_2 (CdS/FTO_{O2}) respectively. Anke et al. [7] showed PL measurements for CdS deposited by CBD; and they described that intermediate orange PL feature centered at 2.00 eV indicates a donor–acceptor recombination and the yellow band observed at 2.12 eV is correlated with (Cd_i–V_{Cd}) complexes. Deep donor Cd_i state density increases due to sulfur deficiency of CdS. Green luminescence bands centered at 2.25 and 2.34 eV are suggested to be transitions from donor levels (e.g., Cd_i states) to the valence band. Shiraki et al. [8] discuss the appearance of red luminescence peak centered at 1.7 eV (4.2 K) with the formation of self-activated centers.

Fig. 2(a) shows SEM images for CdS/FTO_{HCl} as grown; the samples were thermally annealed with $CdCl_2$ ($CdS/FTO_{HCl} + TT_{CdCl2}$), and Ar ($CdS/FTO_{HCl} + TT_{Ar}$) respectively (see Fig. (2b) and (d)); apparently the morphology did not change compared with the CdS as grown. On the other hand Fig. 2(c) corresponds to SEM micrograph of CdS thin films thermally annealed in muffle ($CdS/FTO_{HCl} + TT_{muffle}$); in this

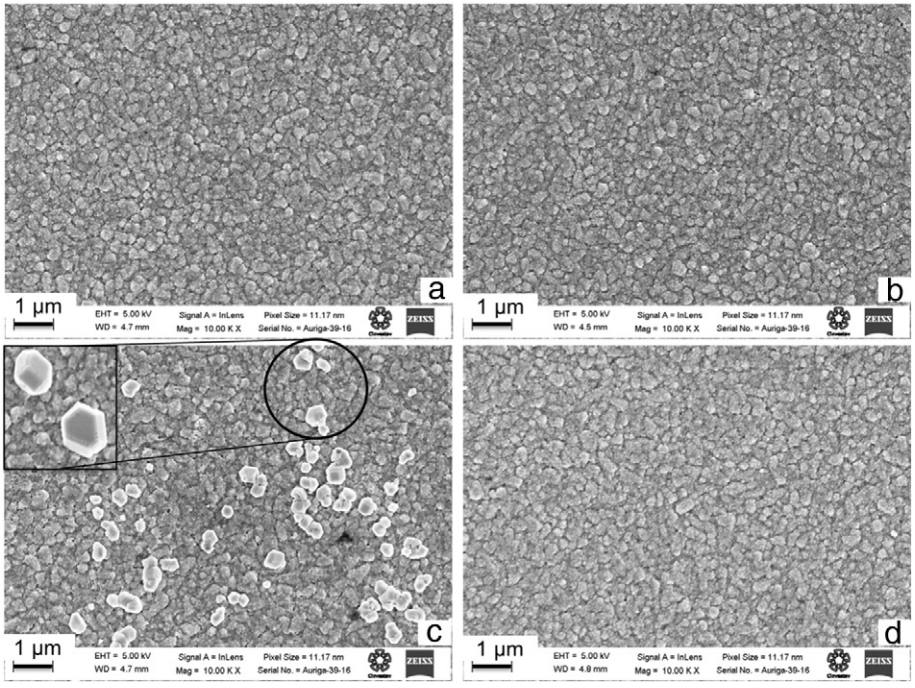

Fig. 2. SEM images at 5 eV; (a) CdS/FTO_{HCl}, (b) $CdS/FTO_{HCl} + TT_{CdCl2}$, (c) $CdS/FTO_{HCl} + TT_{muffle}$ and (d) $CdS/FTO_{HCl} + TT_{Ar}$.

Table 1
Elemental concentrations in the studied CdS thin films.

Sample	[Cd] (at.%)	[S] (at.%)	[Sn] (at.%)	[O] (at.%)	[C] (at.%)
CdS/FTO	12	7	31	44	6
CdS/FTO_{HCl}	10	8	30	45	7
$CdS/FTO_{HCl} + TT_{CdCl2}$	10	8	32	45	5
$CdS/FTO_{HCl} + TT_{muffle}$	12	9	31	44	4
$CdS/FTO_{HCl} + TT_{Ar}$	11	8	31	44	6
[a]$CdS/FTO_{HCl} + TT_{muffle}$	46	1	0	45	8
[b]$CdS/FTO_{HCl} + TT_{muffle}$	8	7	28	44	13

[a] EDS analysis on crystal.
[b] EDS analysis on matrix.

case, some crystals appear on the top of the sample. The subsequent analysis by energy dispersive X-ray spectroscopy (EDS) suggests that these are CdO crystals.

The S/Cd elemental composition of CdS/FTO compared with the CdS/FTO_{HCl} sample was 0.61 and 0.81 respectively; the sulfur quantity in CdS growth increases when the FTO substrate is treated with HCl. The percentage of Cd, S, Sn and O in CdS samples as grown and thermally annealed were determined by EDS measurements (see Table 1). On the other hand, a specific test was made in the matrix and the crystals for the $CdS/FTO_{HCl} + TT_{muffle}$ sample, obtaining crystals conformed by Cd and O. The formation of CdO is promoted by the presence of air inside the heat treatment chamber; the Cd migrates from the matrix and is oxidized, while the sulfur with negative valence (−2) is not promoted due to the reaction of sulfur oxides formation requires a large activation energy.

The transmittance spectra for all samples have an average transmittance value of 87% (see inset in Fig. 3). Energy band gap value was determined; 2.54 eV for the CdS/FTO_{HCl} and $CdS/FTO_{HCl} + TT_{Ar}$ samples (see Fig. 3(a, d)) and 2.43 eV for the $CdS/FTO_{HCl} + TT_{muffle}$ and $CdS/FTO_{HCl} + TT_{CdCl2}$ samples (see Fig. 3(c,b)).

3.2. Crystalline properties.

A typical θ–2θ GI-XRD pattern of CdS thin film with (002), (112) and (004) crystalline orientations identified with PDF-41-1049 star quality is shown in Fig. 4(a, b). Fig. 4(c) shows a structural modeling of CdS. The CdS/FTO_{HCl}, $CdS/FTO_{HCl} + TT_{CdCl2}$ and $CdS/FTO_{HCl} + TT_{Ar}$ samples showed a similar XRD pattern; in this way these three samples are represented in Fig. 4(a). On the other hand, Fig. 4(b) shows a $CdS/FTO_{HCl} + TT_{muffle}$ sample; in this case additional peaks related with CdO appear (see inset in Fig. 4), and the (111) and (311) crystalline orientations were identified with PDF-5-0640 star quality.

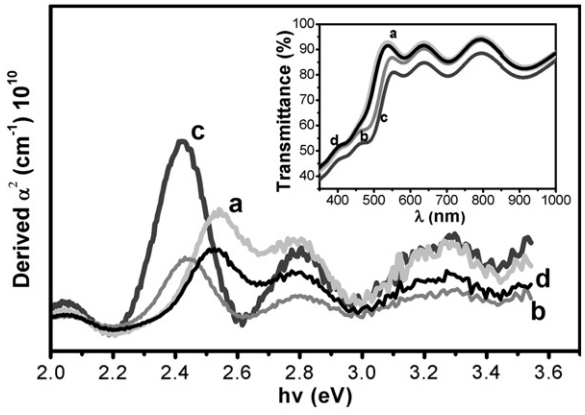

Fig. 3. Derivative absorbance and transmittance spectra (inset); (a) CdS/FTO_{HCl}, (b) $CdS/FTO_{HCl} + TT_{CdCl2}$, (c) $CdS/FTO_{HCl} + TT_{muffle}$ and (d) $CdS/FTO_{HCl} + TT_{Ar}$.

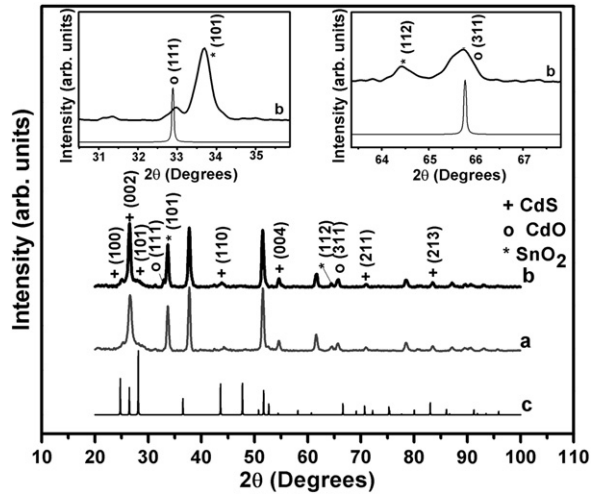

Fig. 4. GI-XRD pattern; (a) CdS/FTO_{HCl}, $CdS/FTO_{HCl} + TT_{CdCl2}$ and $CdS/FTO_{HCl} + TT_{Ar}$, (b) $CdS/FTO_{HCl} + TT_{muffle}$ and (c) CdS modeling.

3.3. Electrical properties.

The CdS/CdTe solar cells were processed in order to evaluate the conversion efficiency using the obtained CdS thin films. Fig. 5(a–f) shows the characteristic I–V curves of the CdS/CdTe cells; the conversion efficiency increases from 4.3 % to 12%. Short-circuit current density (J_{sc}) and open-circuit voltage (V_{oc}) values for the $CdS/FTO_{HCl} + TT_{muffle}$/CdTe configuration in general are higher than the others (see Table 2); on the other hand CdTe solar cells processed with CdS/FTO_{HCl} improve the conversion efficiency (see Fig. 5(a, b)) from 8.7% to 12%. CdTe solar cells were processed using CdS/FTO_{HCl} thin films thermally annealed in muffle, $CdCl_2$ and Ar (see Fig. 5(b, d, f) respectively; we obtained that the thermal treatment in muffle presents the best conversion efficiency value (12%). Fig. 5(a, c, e) shows the CdS/FTO_{Ar} samples thermally annealed in muffle, $CdCl_2$ and Ar respectively; the I vs V measurements reveal that the conversion efficiency increase from 4.3% to 8.7% when CdS/FTO_{Ar} samples are thermally annealed in muffle at atmospheric ambient. The best CdTe solar cell (12%) was obtained using the $CdS/FTO_{HCl} + TT_{muffle}$ configuration; in this case CdO appear on the surface of CdS; CdO causes that series and shunt resistance (R_s) and (R_p) values decrease and increase respectively compared with the $CdS/FTO_{Ar} + TT_{Ar}$ configuration (in the last case CdO did not appear on the surface of CdS) (see Table 2).

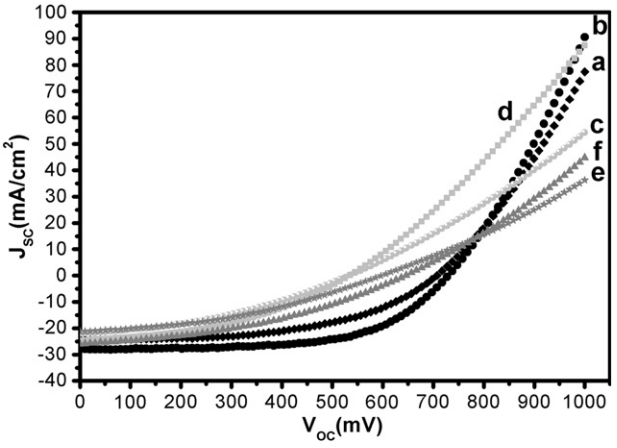

Fig. 5. I vs. V characteristics of CdTe solar cells using; (a) ($CdS/FTO_{Ar} + TT_{muffle}$), (b) ($CdS/FTO_{HCl} + TT_{muffle}$), (c) ($CdS/FTO_{Ar} + TT_{CdCl2}$), (d) ($CdS/FTO_{HCl} + TT_{CdCl2}$), (e) ($CdS/FTO_{Ar} + TT_{Ar}$) and (f) ($CdS/FTO_{HCl} + TT_{Ar}$).

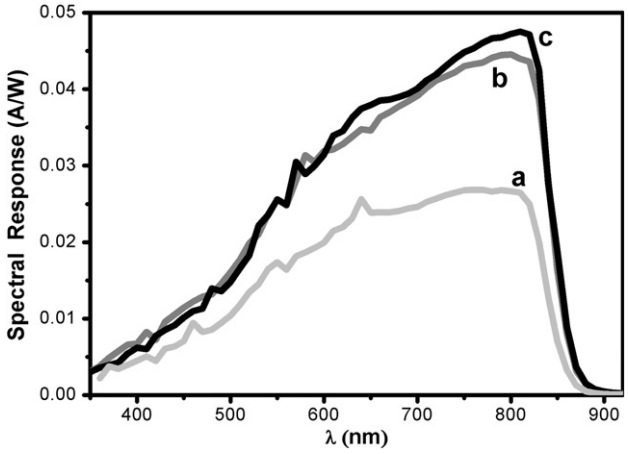

Fig. 6. Spectral response of CdTe solar cells: (a) ($CdS/FTO_{HCl} + TT_{Ar}$), (b) ($CdS/FTO_{Ar} + TT_{muffle}$) and (c) ($CdS/FTO_{HCl} + TT_{muffle}$).

Table 2
Photovoltaic parameters of the studied CdS/CdTe solar cells.

Sample	R_s (Ω-cm^2)	R_p (Ω-cm^2)	V_{OC} (mV)	J_{SC} (mA/cm^2)	FF(%)	η (%)
a	5.5	769	707	25	52	8.7
b	3.2	790	730	28	61	12.0
c	7.4	118	533	22	38	4.3
d	6.1	137	535	25	41	5.3
e	8	123	598	22	39	4.8
f	7.0	305	645	26	40	6.4

Fig. 6 shows the spectral responses of better CdS/CdTe processed solar cells. The short-wavelength cutoff of the spectral response is defined by the absorption edge of CdS, while the long-wavelength edge by the collection of photocurrent from CdTe (including $CdTe_{1-x}S_x$). For the different thermal treatments the variation in the photoelectron collection corresponds with the values of the short current density, and the behavior in the short-wavelength region depends on the kind of thermal treatment on CdS and in the long-wavelength region is influenced by thermal treatments on CdS (see Fig. 6(a, c)) and not entirely by the thermal treatment used on FTO (see Fig. 6(b, c)).

We assume that the shifts in the long wavelength region are a clear evidence of the different thermal treatments. This fact influences the sulfur diffusion into CdTe–interface layer, with the subsequent formation of the $CdTe_{1-x}S_x$ ternary alloy, which as it has been shown before it presents different spectral response in the long wavelength region [9].

4. Conclusions

CdS thin films were deposited by using CBD technique, the FTO substrates used were treated with HCl and others were annealed using different atmospheres (Ar and O_2). All CdS samples showed transmittance values around to 85–91%. The sulfur quantity in CdS growth increases when the FTO substrate is treated with HCl. Photoluminescence measurements reveal that the CdS/FTO_{Ar} presents band-to-band transitions which correspond to a CdS sample with good optical properties; on the other hand, structural and morphological measurements reveals that the $CdS/FTO_{HCl} + TT_{muffle}$ sample presents CdO crystals on the surface of CdS. The series and shunt resistance values decrease and increase respectively when CdO crystals appear on the surface of CdS. The best CdTe solar cell (12%) was obtained using $CdS/FTO_{HCl} + TT_{muffle}$ configuration; in this case CdO appears on the surface of CdS.

Acknowledgments

This work was sponsored by IPN (SIP 20140460, SIP 20140501, SIP20140549) and CONACyT FOMIX 2012-2 number 189282. Special thanks to LANE-CINVESTAV for SEM and EDS measurements, M. Sc. Adolfo Tavira for GI-XRD measurements and CNMC-IPN for their contribution to this work.

References

[1] M.L. Albor Aguilera, J.M. Flores Márquez, M.A. González Trujillo, Y. Matsumoto Kuwahara, G. Rueda Morales, O. Vigil Galán, Influence of CdS thin films growth related with the substrate properties and conditions used on CBD technique, Energy Procedia 44 (2014) 111.
[2] First solar sets world record for CdTe solar cell efficiency, http://investor.firstsolar.com/releasedetail.cfm?ReleaseID=828273.
[3] M.A. Green, K. Emery, Y. Hishikawa, W. Warta, E.D. Dunlop, Solar cell efficiency tables (version 39), Prog. Photovolt. Res. Appl. 20 (2012) 12.
[4] A. Morales Acevedo, Can we improve the record efficiency of CdS/CdTe solar cells? Sol. Energy Mater. Sol. Cells 90 (2006) 2213.
[5] P. Jackson, D. Hariskos, R. Wuerz, W. Wischmann, M. Powalla, Compositional investigation of potassium doped Cu(In, Ga)Se_2 solar cells with efficiencies up to 20.8%, Phys. Status Solidi 8 I (3) (2014) 219.
[6] T.K. Todorov, J. Tang, S. Bag, O. Gunawan, T. Gokmen, Y. Zhu, D.B. Mitzi, Beyond 11% efficiency: characteristic of state-of-the-art $Cu_2ZnSn(S, Se)_4$ solar cells, Adv. Energy Mater. 3 (2013) 34.
[7] Anke E. Abken, D.P. Halliday, Ken Durose, Photoluminescence study of polycrystalline photovoltaic CdS thin film layers grown by close-spaced sublimation and chemical bath deposition, J. Appl. Phys. 105 (2009) 064515.
[8] Y. Shiraki, T. Shimada, K.F. Komatsubara, Optical studies of deep-center luminescence in CdS J, Appl. Phys. 45 (1974) 3554.
[9] A. Romeo, H. Zogg, A.N. Tiwari, in: J. Schmid, H.A. Ossenbrick, P. Helm, H. Ehmann, E.D. Dunlop (Eds.), Proceedings of the 2nd World Conference and Exhibition on Photovoltaic Solar Energy Conversion, Vienna, Austria, 6–10 July, Eur. Comm., 1998, p. 1105.